Vacuum 86 (2012) 594–598

Contents lists available at ScienceDirect

Vacuum

journal homepage: www.elsevier.com/locate/vacuum

Role of the nature of support on the structure of Au–Rh bimetallic nanoparticles

J. Kiss [a,*], A. Oszkó [b], G. Pótári [b], A. Erdőhelyi [a,b]

[a] Reaction Kinetics Research Laboratory, Chemical Research Center of the Hungarian Academy of Sciences, Hungary
[b] Department of Physical Chemistry and Material Science, University of Szeged, Aradi vértanuk tere 1, H-6701 Szeged, P.O.Box 168, Hungary

Keywords:
Titania nanowire
Gold
Rhodium
Bimetallic
Alumina
Core-shell structure

A B S T R A C T

Au, Rh, and Au–Rh clusters were studied on Al_2O_3, TiO_2 powders and titania nanowire by X-ray photoelectron spectroscopy (XPS), scanning electron microscopy (SEM) and infrared spectroscopy (FTIR). On the XP spectra of the Au–Rh/TiO_2 and Au–Rh/Al_2O_3 powders and wires the binding energy of the Au 4f emission was practically unaffected by the presence of Rh, the position of Rh 3d remained also constant on alumina, while it shifted to lower binding energy with gold admixture on titania. New emission for Rh 3d at 309.2 eV and for Au 4f at 85.6 eV developed on titania wire case. The bands due to Rho-CO and $(Rho)_2$–CO were observed on IR spectra of titania supported bimetallic samples. The peak due to Rh^+–$(CO)_2$ was less intense on bimetallic nanowire. All three bands however are intense on Au–Rh/Al_2O_3. The results were interpreted by electron donation from titania through gold to rhodium. "Core-shell" bimetallic structures are supposed on Au–Rh/titania wire.

1. Introduction

Since most heterogeneous catalysts consist of metal clusters on oxide supports, it is important to understand the nature and effect of cluster–support interactions. Titania based supports have recently become the subject of renewed interest, since gold clusters on TiO_2 have been found to exhibit unique catalytic properties, which are absent on other supports [1,2]. Titania supports are known to be highly reducible and undergo strong metal support interactions with metals, including Rh, Pt, Ni [3,4]. It is frequently observed that the presence of a second metal can greatly influence the catalytic behavior of gold. Enhanced dispersion and stability of gold nanoparticles on stoichiometric and reduced TiO_2(110) was observed in the presence of molybdenum [5]. Sintering of Au-containing clusters on titania is suppressed by the presence of Pt in Au-Pt bimetallic clusters [6]. It has also been observed that Rh significantly changed the morphology and topology of Au on TiO_2(110) surface [7,8]. STM and LEIS experiments revealed that proper Au and Rh coverage, the post deposited Au covers completely and uniformly the Rh nanoparticles.

It is well known that the nature of the support greatly influences the surface processes. Titanium oxide nanostructures (wire and tube) have attracted considerable attention lately because of their numerous potential applications in solar cells [9], electronics [10], photocatalysis [11], sensorics [12] and as catalysts support [13]. Ordered TiO_2 nanostructures can be obtained by hydrothermal conversion of anatase [14,15]. In this paper we study the structure and morphology of gold-rhodium bimetallic nanoparticles on titania nanowire by X-ray photoelectron spectroscopy, scanning electron microscopy and infrared spectroscopy. The results obtained on nanowire are compared to Au–Rh/TiO_2 and alumina supported bimetallic system.

2. Experimental

Preparation of titania nanowire was described elsewhere [15]. It was characterized by TEM. Au, Rh and their coadsorbed layers with three different compositions were produced by impregnating TiO_2 (Degussa P25), titania nanowire and γ–Al_2O_3 (Degussa P110CI) with mixtures of calculated volumes of $HAuCl_4$ (Fluka) and $RhCl_3x3H_2O$ (Johnson Matthey) solution to yield 1 wt % metal content. The impregnated powders were dried in air at 383 K for 3 h. The final pre-treatment was at 573 K in hydrogen atmosphere [16].

Scanning electron microscopy (SEM) was done on a Hitachi S-4700 field emission scanning electron microscope equipped with Röntec energy dispersive X-ray spectrometer. Transmission electron microscopic (TEM) observations were performed on a Philips CM10 instrument using copper mounted holey carbon grids. The specific surface area was calculated using BET method from N_2 adsorption isotherms measured at 77 K on a Quantachrome NOVA 2000 instruments. The diameter of titania nanowire is 45–110 nm

* Corresponding author.
E-mail address: jkiss@chem.u-szeged.hu (J. Kiss).

0042-207X/$ – see front matter © 2011 Elsevier Ltd. All rights reserved.
doi:10.1016/j.vacuum.2011.07.014

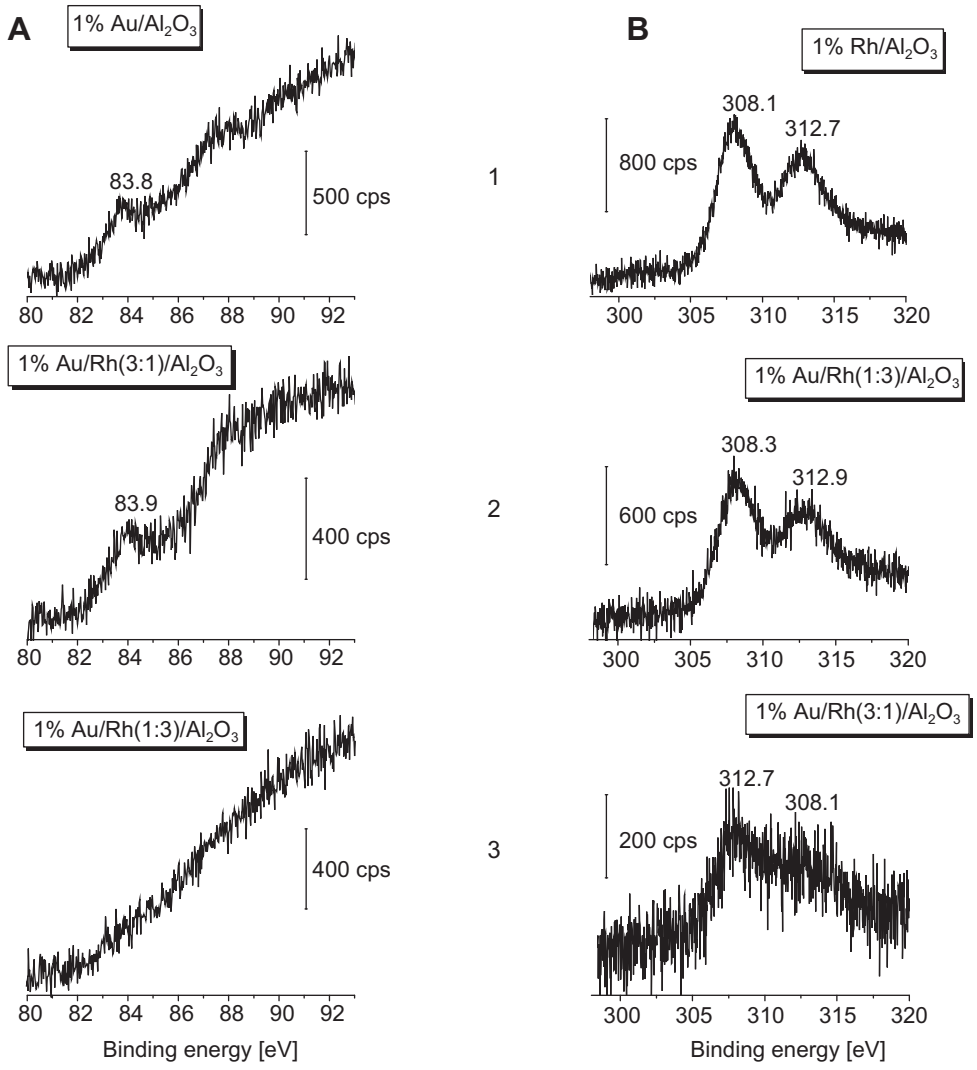

Fig. 1. (A) - Au 4f regions of XP spectra of reduced sample: 1–1% Au/Al_2O_3, 2–0.75% Au + 0.25% Rh/Al_2O_3, 3–0.25% Au + 0.75% Rh/Al_2O_3; (B) Rh 3d regions of XP spectra: 1–1% Rh/Al_2O_3, 2–0.75% Rh + 0.25% Au/Al_2O_3, 3–0.25% Rh + 0.75% Au/Al_2O_3.

and their length is between 1.8 and 5 μm. The specific surface area of nanowires is $\sim$20 $m^2\ g^{-1}$.

XP spectra were taken with an SPECS instrument equipped with a PHOIBOS 150 MCD 9 hemispherical analyzer. The analyzer was operated in the FAT mode with 20 eV pass energy. The Al K_α radiation ($h\nu = 1486.6$ eV) of a dual anode X-ray gun was used as an excitation source. The gun was operated at 150 W power (12.5 kV, 12 mA). The energy step was 25 meV, electrons were collected for 100 ms in one channel. Typically five scans were summed to get a single high resolution spectrum.

For binding energy reference the usually complex C 1s spectrum was first deconvoluted and the peak maximum of the appropriate synthetic component was fixed at 285.1 eV. In other cases either the Al 2p spectrum envelope (Al 2p at 74.7 eV) or the Ti $2p_{3/2}$ maximum (458.9 eV) was used as energy reference. For spectrum acquisition and evaluation both manufacturer's (SpecsLab2) and commercial (CasaXPS, Origin) software packages were used. For IR studies the catalysts powders were pressed onto Ta-mesh. The mesh was fixed to the bottom of a conventional UHV sample manipulator. It was resistively heated and the temperature of the sample was measured by NiCr–Ni thermocouple spot welded directly to the mesh. IR spectra were recorded with Genesis (Mattson) FTIR spectrometer. The whole optical path was purged with a Balston 75-62 FT–IR purge generator.

3. Results and discussion

After recording the X-ray photoelectron spectra of as-received sample in vacuum, the catalysts were reduced in the preparation chamber in H_2 for 1 h then H_2 was evacuated at 573 K; this followed by cooling down to room temperature and transporting of the samples to the measuring chamber for obtaining the XP spectra of reduced catalysts. The positions of Al 2p, Ti 2p and O 1s peaks remained unaltered after reduction. No appreciable change in the position of Au 4f emission was recorded on the spectra of reduced Au-containing samples in comparison with the as-received catalysts. In the case of Rh 3d the observed XP spectra of the as-received sample shifted to lower binding energy after reduction. In the case of alumina this value was at 308.0 eV. The position was practically the same on bimetallic (Au + Rh) alumina powder, too (Fig. 1). This observation shows that there are not significant interactions between Au and Rh on Al_2O_3.

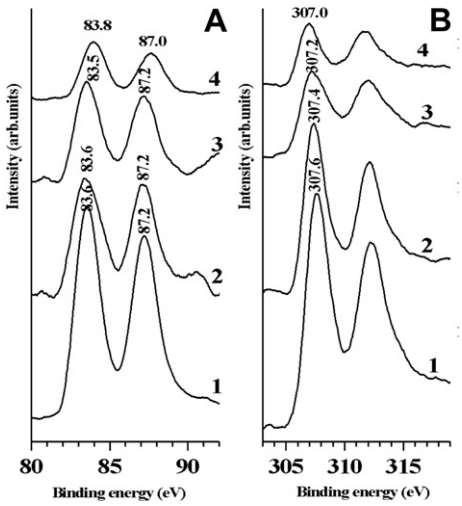

Fig. 2. XPS obtained on powdered titania (A) - Au 4f regions of XP spectra of reduced sample; 1–1% Au/TiO_2, 2–0.75% Au + 0.25% Rh/TiO_2, 3–0.5% Au + 0.5% Rh/TiO_2, 4–0.25% Au + 0.75% Rh/TiO_2 (B) – Rh 3d region of XP spectra; 1–1% Rh/TiO_2, 2–0.75% Rh + 0.25% Au/TiO_2, 3–0.5% Au + 0.5% Rh/TiO_2, 4–0.25% Rh + 0.75% Au/TiO_2.

The situation was different on Degussa TiO_2 compared to Al_2O_3 support. After reduction we measured a Rh 3d binding energy of 307.6 eV, which corresponds to a reduced state in high dispersion (Fig. 2B). A continuous shift with Au content to lower binding energy in the position of Rh 3d of reduced sample, however, can clearly be recognized. This tendency may indicate that the particle size became larger, more metallic. Our recent data on acetonitrile adsorption on Au/TiO_2 [17] and on Rh/TiO_2 [18] revealed that an electron flow is directed from TiO_2 to metal.

More complex picture was observed on titania nanowire. In the case of 1% Au/TiO_2 nanowire two binding energy peaks were observed on clean reduced sample for Au 4f at 83.7 eV (metallic state) and 85.6 eV (Fig. 3A). The emission at 85.6 eV cannot be attributed to a kind of higher oxidation sites because it developed after hydrogen treatment at 573 K. We may attribute this feature to the particles in very small nanosize (final state effect). This atomically-dispersed state was also observed with Au atoms complexed to oxygen vacancy on TiO_2(110) at low temperature [19]. On monometallic Rh/TiO_2 nanowire the dominant XPS peak appeared after reduction at 573 K for Rh 3d at 307.1 eV (Fig. 3B). A careful deconvolution revealed some emission at 309.2 eV, presumably due to more dispersed nanoparticles. This feature significantly increased after CO adsorption du to CO induced disruption of Rh

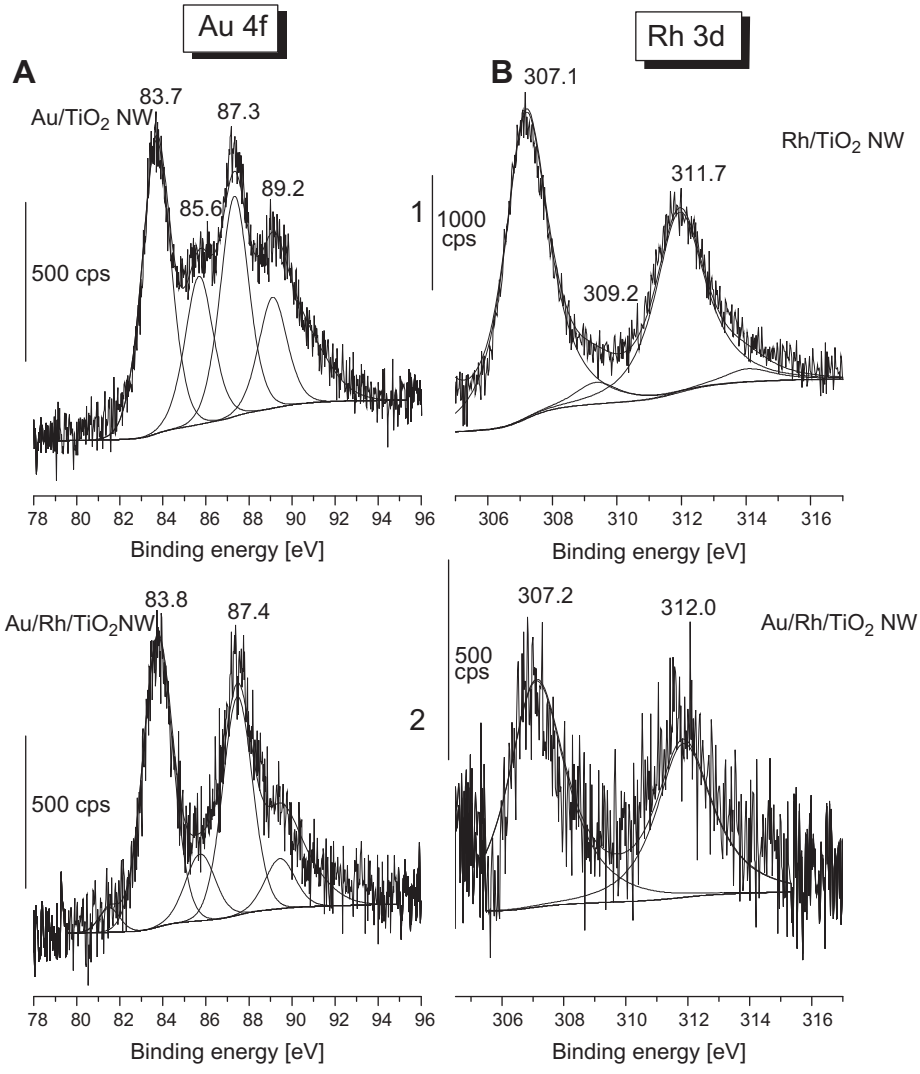

Fig. 3. XPS obtained on titania nanowire (A) – Au 4f region, 1–1% Au, 2–0.5% Au + 0.5% Rh; (B) Rh 3d region, 1–1% Rh, 2–0.5% Au + 0.5% Rh.

(not shown). XP spectra of bimetallic Au + Rh layer supported on titania nanowire are also shown in Fig. 3. Surprisingly the emission for higher energy peak of Au 4f at 85.6 eV for atomically-dispersed state significantly decreased or disappeared, in the presence of Rh (Figs. 2 and 3A) and the same time some emission for Rh 3d at 309.2 eV diminished (Figs. 2 and 3B). These changes indicate that interaction between small nanosizes of the Au and Rh occurred. The cluster sizes are increased.

Infrared spectra of adsorbed species are frequently used as a fingerprint technique to identify the morphological and chemical states of active metals on supported oxides. Adsorbed CO exhibits at least three different stretching frequencies belonging to the certain adsorption states of Rh on oxide supports [20–22]. In addition to this CO caused the disruption of rhodium clusters [22]. Recently the disruption of Rh to smaller size particles was confirmed by STM [23]. The band at 2070–2030 cm^{-1}, depending on the coverage, is due to CO adsorbed linearly to Rho, the band at ~1855 cm^{-1} represents the bridge bonded CO (Rh_2–CO), and the feature at ~2100 cm^{-1} and at ~2020 cm^{-1} corresponds to the symmetric and asymmetric stretching of $Rh^{+}(CO)_2$ (twin CO). This latest IR signals were detected when the crystallite size was very small [22]. On alumina supported Rh, and bimetallic Au + Rh all the three adsorbed form are developed in FTIR spectra (Fig. 4A). CO adsorbed on gold was not observed. On rhodium supported titania nanowire the dominant or sole species was the twin (geminal) CO at 2028 and 2097 cm^{-1}. With increasing gold content, however, the linear form became stronger at 2073 cm^{-1} and the twin CO stretching frequency was relatively less in intensity (Fig. 4B). CO adsorption on gold supported by titania nanowire was not observed. These IR results also suggest that the particle size of the bimetallic cluster became larger. On the other hand, the large mean free path of surface diffusion of gold (mainly in smallest size) on the titania wire allows accumulation of Au on the Rh seeds, blocked the formation of twin CO. This type of bimetallic structure (core-shell) was predicted on Au–Rh/TiO_2(110) surface [8], too. SEM data are also showing an increase in size. The average diameter of monometallic Au and Rh nanoparticles is 8 and 6 nm, respectively. In the bimetallic cluster the average diameter is around 13 nm.

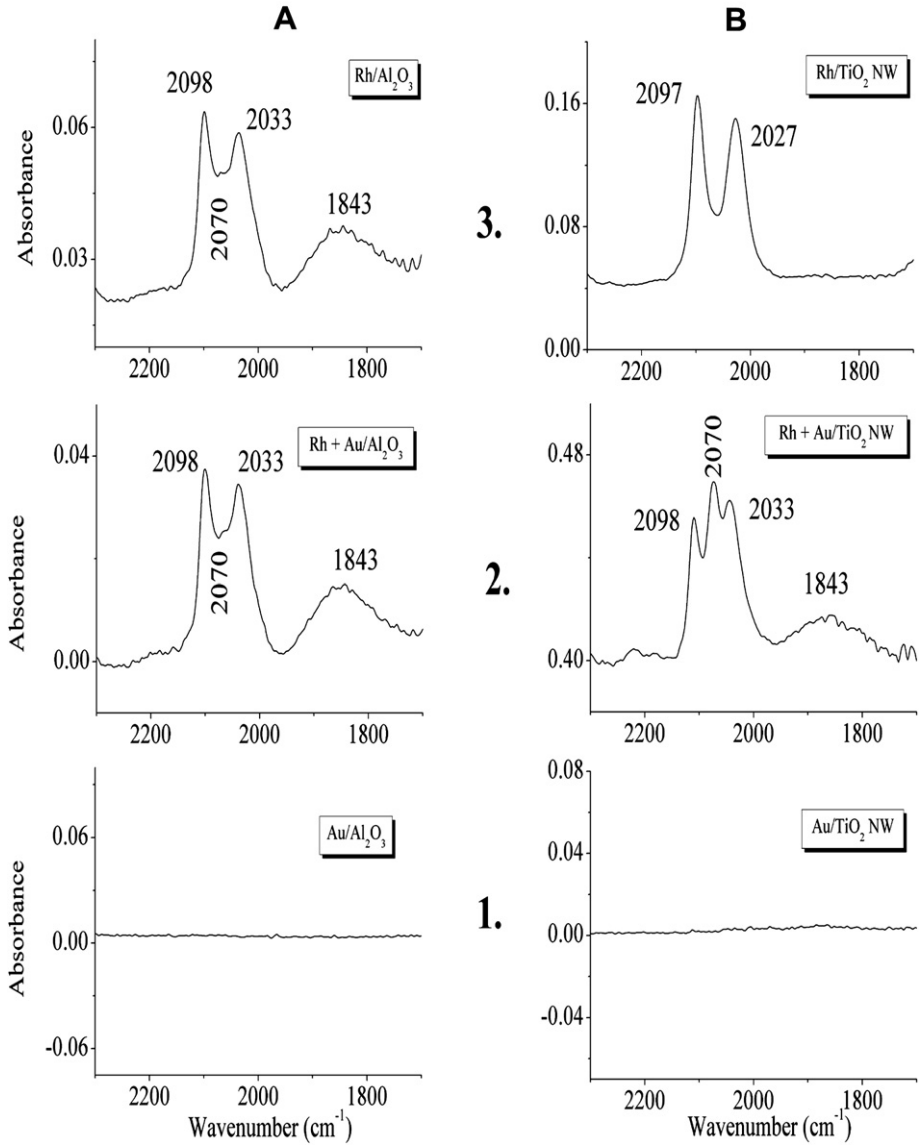

Fig. 4. IR spectra after CO adsorption (A) on Al_2O_3; 1–1% Au, 2–0.5% Au + 0.5% Rh, 3–1% Rh; (B) on titania nanowire; 1–1% Au, 2–0.5% Au + 0% Rh, 3–1% Rh. T = 300 K, P_{co} = 1.3 mbar.

4. Conclusion

1. Monometallic gold and rhodium nanoclusters exhibit well dispersed system on Al_2O_3. XP spectra give single peaks for Au $4f_{7/2}$ and Rh $3d_{3/2}$ emissions. CO does not adsorb on gold at 300 K, on Rh/Al_2O_3, however twin, linear and bridge bonded CO vibrations were observed. In bimetallic Au–Rh system, no significant interactions were detected between metals on alumina.
2. On TiO_2 nanowire support the gold $4f_{7/2}$ XP emission appeared at after reduction at 83.6 eV and 85.6 eV indicating two different size or chemical environment in gold nanoclusters. For rhodium small cluster size also observed after reduction at 309.2 eV besides of clean metallic state at 307.1 eV. CO adsorption on 1% Rh/TiO_2 nanowire caused dominant stretching frequencies for twin (geminal) form.
3. On bimetallic nanosystem the linear CO stretching frequency was the highest, at the same time the highest binding energy states on reduced sample almost diminished indicating the enlargement of nanocluster. Very likely “core-shell” bimetallic clusters form, in which the gold covers the rhodium.

Acknowledgement

The Hungarian Scientific Research Foundation Grant OTKA (K81660, K69200, K76489) supported this work. The authors thank gratefully for the valuable discussions and preparation of titania naniwire to Drs. Zoltán Kónya and Ákos Kukovecz.

References

[1] Haruta A. Chem Rec 2003;3:75.
[2] Haruta M. Cattech 2002;6:102.
[3] Solymosi F. Catal Riew 1968;1:233.
[4] Tauster SJ. Acc Chem Res 1987;20:389.
[5] Bugyi L, Berkó A, Óvari L, Kiss AM, Kiss J. Surf Sci 2008;602:1650.
[6] Park JB, Conner SF, Chen DA. J Chem. C 2008;112:5490.
[7] Óvari L, Bugyi L, Zs Majzik, Berkó A, Kiss J. J Phys Chem C 2008;112:1811.
[8] Óvari L, Berkó A, Balázs N, Zs Majzik, Kiss J. Langmuir 2010;26:2167.
[9] O'Regan B, Gratzel M. Nature (London) 1991;353:737.
[10] Croce F, Appetecchi GB, Persi L, Scrosati B. Nature (London) 1998;394:456.
[11] Hodos M, Horváth E, Haspel H, Kukovecz Á, Kónya Z, Kiricsi I. Chem Phys Lett 2004;399:512.
[12] Mor GK, Carvalho MA, Varghese OK, Pishko MV, Grimes CA. J Mater Res 2004; 19:628.
[13] Valden M, Lai X, Goodman DW. Science 1998;281:1647.
[14] Kukovecz Á, Hodos M, Horváth E, Radnóczi Gy, Kónya Z, Kiricsi I. Phys Chem B 2005;109:17781.
[15] Horváth E, Kukovecz Á, Kónya Z, Kiricsi I. Chem. Mater 2007;19:927.
[16] Kiss J, Németh R, Koós A, Raskó J. J Nanosci Nanotechnol 2009;9:3828.
[17] Raskó J, Kiss J. Catal Lett. 2006;109:71.
[18] Raskó J, Kiss J. Appl.Catal A Gen 2006;303:56.
[19] Fan C, Wu T, Anderson SL. Surf Sci 2005;578:5.
[20] Prime M. J.Chem Soc Faraday Trans 1978;74:2571.
[21] Rice CA, Worley SD, Curtis CW, Guin JA, Tarrer AR. J Chem Phys 1981;74:6748.
[22] Solymosi F, Pásztor M. J Phys Chem 1985;89:4783.
[23] Berkó A, Solymosi F. J Catal 1999;183:91.